Proton NMR study of α-MnH$_{0.06}$

A.V. Soloninin[a], A.V. Skripov[a,*], A.L. Buzlukov[a], V.E. Antonov[b], T.E. Antonova[b]

[a]*Institute of Metal Physics, Urals Branch of the Russian Academy of Sciences, S. Kovalevskoi 18, 620219 Ekaterinburg, Russian Federation*
[b]*Institute of Solid State Physics, Russian Academy of Sciences, 142432 Chernogolovka, Russian Federation*

Abstract

Proton nuclear magnetic resonance (NMR) spectra and spin–lattice relaxation rates for the solid solution α-MnH$_{0.06}$ have been measured over the temperature range 11–297 K and the resonance frequency range 20–90 MHz. A considerable shift and broadening of the proton NMR line and a sharp peak of the spin–lattice relaxation rate are observed near 130 K. These effects are attributed to the onset of antiferromagnetic ordering below the Néel temperature $T_N \approx 130$ K. The proton NMR line does not disappear in the antiferromagnetic phase; this suggests a small magnitude of the local magnetic fields at H-sites in α-MnH$_{0.06}$. The spin–lattice relaxation rate in the paramagnetic phase is dominated by the effects of spin fluctuations.
© 2004 Elsevier Ltd. All rights reserved.

1. Introduction

The maximum solubility of hydrogen in α-manganese increases from about 0.3 at.% at atmospheric pressure to a few atomic percent at hydrogen pressures of 0.6–0.9 GPa [1]. The solid solutions α-MnH$_x$ ($x \leq 0.073$) obtained by high-pressure quenching retain long-term stability at room temperature after the pressure release [2]. The neutron diffraction study of α-MnH$_{0.07}$ [2] has shown that H atoms randomly occupy the interstitial sites 12e of the space group $I\bar{4}3m$ in the complex cubic unit cell of α-Mn composed of 58 manganese atoms. The sublattice of 12e sites consists of dumb-bells of closely-spaced sites, the distance between the sites in a dumb-bell being only 0.68 Å. Inelastic neutron scattering studies of α-MnH$_{0.07}$ have revealed a strong splitting of about 6.4 meV of the vibrational ground state of hydrogen due to tunneling between the sites in a dumb-bell [2,3]. Because of the large energy of the tunneling modes,

hydrogen tunneling in α-MnH$_{0.07}$ dominates over the thermal diffusion at temperatures up to 140 K [3], as compared to 5–10 K for any other metal–hydrogen system [4,5].

Below the Néel temperature $T_N = 95$ K, α-Mn is ordered antiferromagnetically and has a complex non-collinear magnetic structure with six inequivalent sites ([6] and references therein). The transition into the antiferromagnetic phase is accompanied by a tetragonal distortion of the lattice. The ^{119}Sn Mössbauer investigation [7] has shown that hydrogenation of α-Mn containing 0.2 at.% Sn leads to a considerable increase in the Néel temperature from 97.3 K for the hydrogen-free sample to 128.3 K for the solid solution with 5 at.% H.

In this Communication we report the results of the first nuclear magnetic resonance (NMR) experiments in α-MnH$_x$. We have measured the proton NMR spectra and spin–lattice relaxation rates for the powdered sample of α-MnH$_{0.06}$ over the temperature range 11–297 K including the regions of the occurrence and absence of hydrogen tunneling and antiferromagnetic ordering.

* Corresponding author. Tel.: +7-343-378-3781; fax: +7-3-433-745-244.

E-mail address: skripov@imp.uran.ru (A.V. Skripov).

2. Experimental details

A 3.1 g sample of a solid solution α-MnH$_x$ was prepared by an exposure of freshly powdered manganese metal of 99.99 wt% purity to a hydrogen pressure of 0.8 GPa at 623 K for 4 h; details of the technique are described in Ref. [1]. This solution was thermally stable under ambient conditions; noticeable hydrogen losses were observed at heating above approximately 350 K. The hydrogen content ($x = 0.059 \pm 0.002$) was determined by hot extraction into a calibrated volume at temperatures up to 800 K. X-ray diffraction analysis at room temperature has shown that the sample is a single-phase solid solution retaining the host-metal structure of α-Mn with the increased value of the lattice parameter $a = 8.942 \pm 0.005$ Å. This value is in reasonable agreement with the experimental $a(x)$ dependence for α-MnH$_x$(D$_x$) solutions [8] that gives $a(0.059) = 8.935$ Å.

Proton NMR measurements were performed on a modernized Bruker SXP pulse spectrometer at the frequencies $\omega/2\pi = 20$, 23.8, 40 and 90 MHz. The ^{1}H NMR spectra were recorded by Fourier transforming the spin echo signals. For linewidths exceeding 60 kHz, the spectra were obtained by superimposing a number of Fourier spectra excited at different magnetic fields. The spin–lattice relaxation rates R_1 were measured by the saturation-recovery method.

3. Results and discussion

The proton NMR spectra have been recorded at the resonance frequencies of 20 and 90 MHz in the temperature range 82–297 K. For both resonance frequencies, the shape and the width of the proton NMR line remain nearly unchanged in the range 130–297 K. The width of the ^{1}H line in this range is determined mainly by the ^{1}H–^{55}Mn dipole–dipole interaction. In fact, calculation of the 'rigid-lattice' dipolar second moment of the proton NMR line using eight nearest-neighbor H–Mn distances taken from Ref. [2] yields $\langle \Delta \omega^2 \rangle = 1.05 \times 10^{10}$ s^{-2}; for a Gaussian line this corresponds to the full width at half-maximum $\delta = 38.4$ kHz. The experimental values of δ at 297 K are 40 and 54.9 kHz for $\omega/2\pi = 20$ and 90 MHz, respectively.

Below 130 K, the width of the proton NMR line starts to increase rapidly. This broadening is accompanied by a shift of the line maximum and by the appearance of a flat background of considerable intensity. As an example of the data, Fig. 1 shows the evolution of the ^{1}H NMR spectrum at $\omega/2\pi = 20$ MHz in the temperature range 82–130 K. The temperature dependences of the linewidth δ and the relative shift of the line maximum S at $\omega/2\pi = 90$ MHz are shown in Figs. 2 and 3, respectively. Both the additional broadening and the shift of the ^{1}H NMR line can be attributed to the onset of a distribution of local magnetic fields due to
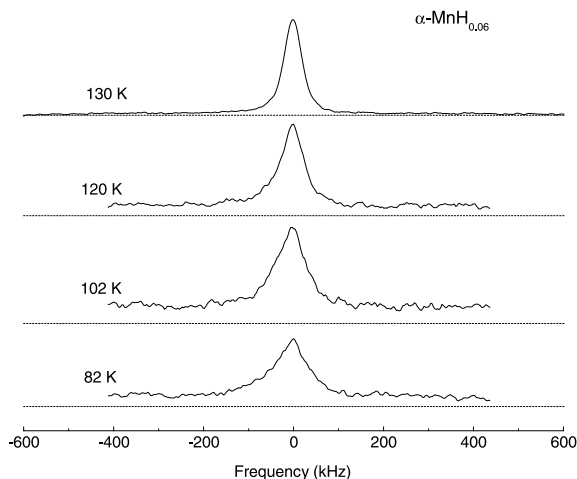

Fig. 1. The evolution of the proton NMR spectrum for α-MnH$_{0.06}$ measured at 20 MHz in the temperature range 82–130 K. The dashed lines show the zero intensity for the corresponding spectra.

antiferromagnetic ordering below $T_N \approx 130$ K. This T_N value agrees with that found for the Sn-doped α-MnH$_{0.05}$ ($T_N \approx 128$ K) by Mössbauer spectroscopy [7].

The α modification of manganese is the only elemental antiferromagnet showing an increase in T_N on hydrogenation (for a review, see Ref. [9]). It is reasonable to assume that this effect can be accounted for in terms of the rigid d-band model [10], since this model semi-quantitatively describes the magnetic properties of all transition-metal hydrides studied so far, including manganese hydrides with h.c.p. (ε) [9] and f.c.c. (γ) [11] metal lattice. According to the rigid d-band model, these properties change with H concentration as if hydrogen were simply donating $\eta \approx 0.5$ electrons per atom into the otherwise unchanged metal d-band. Therefore, the dissolution of $x = 0.06$ hydrogen atoms in α-Mn should increase its effective d-band occupation by $\Delta N_{eff}^e = x\eta \approx 0.03$ electrons per Mn atom. Thus, the
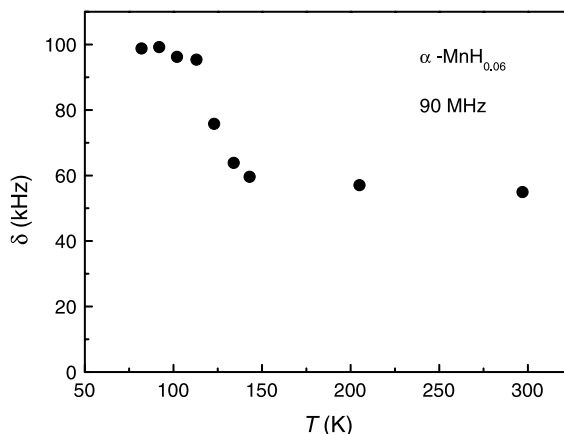

Fig. 2. The temperature dependence of the full width at half-maximum, δ, of the proton NMR line measured at 90 MHz.
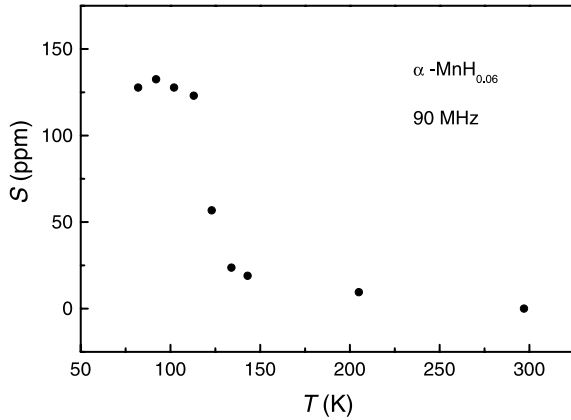
Fig. 3. The temperature dependence of the relative shift, S, of the maximum of the proton NMR line measured at 90 MHz. The shift at $T = 297K$ is taken as zero.

increase in the Néel temperature $\Delta T_N = T_N(x = 0.06) - T_N(x = 0) \approx 130 - 95 = 35$ K corresponds to the average rate of $dT_N/dN_{eff}^e \approx 35/0.03 \approx 1200$ K/electron. This value can be compared with that resulting from the Mössbauer investigation of substitutional alloys α-$Mn_{1-y}Sn_y$ [7]. According to Ref. [7], an increase in the tin concentration from $y = 2.0 \times 10^{-3}$ to $y = 4.2 \times 10^{-3}$ leads to the increase in T_N from 97.3 to 107 K. Alloying of itinerant ferromagnets Co and Ni with Sn and some other non-transition elements is known to change the magnetic properties of the host metal approximately in the same way as an increase in the electron concentration by v electrons per impurity atom, where v is the valence of the impurity [12]. Assuming that this is also valid for Sn in the itinerant antiferromagnet α-Mn, we obtain $dT_N/dN_{eff}^e \approx \Delta T_N/(\Delta y v) \approx 9.7/(2.2 \times 10^{-3} \times 4) \approx 1100$ K/electron. The good agreement between the estimates of dT_N/dN_{eff}^e for two different types of solute elements, hydrogen and tin, suggests that this value may be an intrinsic property of the electronic structure of α-Mn.

It is interesting to note that the ^1H NMR line in α-$MnH_{0.06}$ does not disappear completely in the antiferromagnetic phase. The width of this line does not exceed 100 kHz down to 82 K, and the shift of the line maximum between 82 and 130 K is only about 100 ppm. This means that the local magnetic fields probed by ^1H nuclear spins in the antiferromagnetic phase are quite weak. According to the neutron diffraction data [2], hydrogen atoms at 12e sites are surrounded by Mn atoms at positions 24g_1 and 24g_2 (MnIII and MnIV in the notation of Ref. [6]). The magnetic moments at MnIII and MnIV in the antiferromagnetic phase of α-Mn are found to be small (0.2–0.6 μ_B), as compared to the magnetic moments at MnI and MnII sites (1.8–2.8 μ_B) [6]. Therefore, the weakness of the local magnetic fields at H sites in α-$MnH_{0.06}$ may be ascribed to small magnetic moments at the nearest-neighbor Mn atoms and to a partial cancellation of magnetic fields induced by different Mn

atoms. The temperature dependence of the shift of ^1H NMR line below T_N is expected to reflect the temperature dependence of the staggered magnetization. In fact, as can be seen from Fig. 3, the behavior of the shift below T_N is typical of that for the order parameter of a second-order phase transition. Since the observed shift is rather small, we have not tried to fit its temperature dependence to any theoretical model.

The proton spin–lattice relaxation rates R_1 in α-$MnH_{0.06}$ have been measured at the resonance frequencies $\omega/2\pi = 23.8$, 40 and 90 MHz in the temperature range 11–290 K. Above 130 K the proton spin–lattice relaxation is well described by a single exponential function; the corresponding experimental values of R_1 at three resonance frequencies are shown in Fig. 4. Below 130 K, we have found considerable deviations from the single-exponential relaxation. The data shown in Fig. 4 for $T < 130$ K correspond to the 1/e point on the recovery of nuclear magnetization at 90 MHz. The main feature of the proton relaxation data is the sharp peak of the relaxation rate near 130 K.

In order to discuss the $R_1(T)$ data, we have to clarify the dominant mechanisms of nuclear spin–lattice relaxation. For many metal–hydrogen systems, the nuclear dipole–dipole interaction modulated by hydrogen motion gives the most important contribution to the measured proton R_1 [13]. The characteristic feature of this mechanism is the frequency-dependent $R_1(T)$ maximum occurring at the temperature at which the H jump rate τ^{-1} becomes nearly equal to ω. The amplitude of this maximum is proportional to the fraction of the dipolar second moment that is averaged out by hydrogen motion [14]. Using the estimated value of $\langle \Delta \omega^2 \rangle = 1.05 \times 10^{10}$ s^{-2} for α-MnH_x and assuming that the localized H motion within 12e dumb-bells averages out one-third of $\langle \Delta \omega^2 \rangle$ (which is typical of localized H motion [15]), we find that the maximum dipole–dipole contribution to R_1
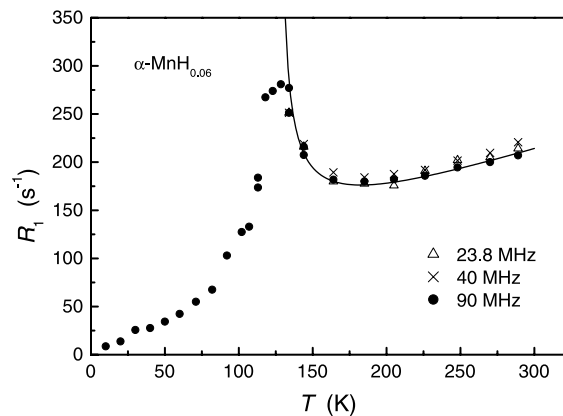

Fig. 4. The temperature dependence of the proton spin–lattice relaxation rate, R_1, for α-$MnH_{0.06}$ measured at 23.8, 40 and 90 MHz. The solid curve represents the fit of Eq. (2) to the data at 90 MHz in the paramagnetic phase.

at $\omega/2\pi = 90$ MHz is 13 s^{-1}. This value is much lower than the measured proton spin–lattice relaxation rates over most of the studied temperature range. Therefore, the proton relaxation rate in α-MnH$_{0.06}$ is dominated by some other relaxation mechanism.

It is known that in metallic systems undergoing magnetic phase transitions the electron–electron interaction leads to a strong enhancement of the nuclear spin–lattice relaxation rate with respect to the usual Korringa value [16,17]. In particular, the relaxation rate is expected to diverge as the transition temperature is approached. A sharp $R_1(T)$ peak near T_N has been observed in a number of weakly antiferromagnetic metals including CrB$_2$ [18] and β-Mn alloys [19,20]. The behavior of $R_1(T)$ for α-MnH$_{0.06}$ resembles that for these systems, taking into account that the value of T_N for α-MnH$_{0.06}$ is close to 130 K. Such a behavior suggests that the dominant mechanism of the proton spin–lattice relaxation in α-MnH$_{0.06}$ is due to the contact hyperfine interaction enhanced by the effects of spin fluctuations [16,17]. This conclusion is also supported by the fact that the measured R_1 above T_N does not show any significant dependence on the resonance frequency (Fig. 4). According to the renormalized spin fluctuation theory of Moriya and Ueda [16,17], in weakly antiferromagnetic metals $R_1(T)$ behaves as

$$R_1 \propto T/(T - T_N)^{1/2} \tag{1}$$

above T_N. In particular, this approach predicts that for $T \gg T_N$ the relaxation rate is proportional to $T^{1/2}$. Although all qualitative features of the observed $R_1(T)$ above T_N can be described by Eq. (1), we have found that a quantitative description of the data requires an additional Korringa-like term cT. Therefore, the expression

$$R_1 = bT/(T - T_N)^{1/2} + cT \tag{2}$$

has been used to fit our $R_1(T)$ data above T_N. Similar approach has been invoked in the case of β-Mn alloys [19], the Korringa-like term being ascribed to the orbital hyperfine interaction [21]. In our case this term is likely to originate from the dipole–dipole hyperfine interaction [21]. The solid line in Fig. 4 shows the fit of Eq. (2) to the $R_1(T)$ data at 90 MHz; the corresponding fit parameters: $T_N = 128$ K, $b = 4.25$ s^{-1} K$^{-1/2}$ and $c = 0.39$ s^{-1} K^{-1}.

Below T_N the theory [16,17] predicts that R_1 is proportional to $T/M(T)$ where $M(T)$ is the staggered magnetization. The observed behavior of the relaxation rate below T_N (Fig. 4) is in qualitative agreement with this prediction. However, because of the deviations from the single-exponential relaxation below T_N, we have not tried to fit the data in this temperature range.

4. Conclusions

Our proton NMR study of the solid solution α-MnH$_{0.06}$

prepared at high hydrogen pressure has revealed a marked shift of the line and a sharp peak of the spin–lattice relaxation rate near 130 K. These effects are attributed to the transition of α-MnH$_{0.06}$ into antiferromagnetic state at $T_N \approx 130$ K, which is considerably higher than $T_N \approx 95$ K for the hydrogen-free α-Mn. It has been found that the temperature dependence of the measured proton spin–lattice relaxation rate is in agreement with the predictions of the renormalized spin fluctuation theory [12,13]. This suggests that R_1 in α-MnH$_{0.06}$ is dominated by the effects of spin fluctuations. We have not found any significant contributions to R_1 due to the fast localized H motion within 12e dumb-bells.

The local magnetic fields probed by ^{1}H nuclei in the antiferromagnetic phase of α-MnH$_{0.06}$ appear to be weak. Details of the magnetic structure of α-MnH$_x$ may be clarified by zero-field ^{55}Mn NMR measurements in the antiferromagnetic phase. Such measurements are in progress now.

References

[1] V.E. Antonov, T.E. Antonova, N.A. Chirin, E.G. Ponyatovsky, M. Baier, F.E. Wagner, Scr. Mater. 34 (1996) 1331.

[2] V.K. Fedotov, V.E. Antonov, K. Cornell, G. Grosse, A.I. Kolesnikov, V.V. Sikolenko, V.V. Sumin, F.E. Wagner, H. Wipf, J. Phys.: Condens. Matter 10 (1998) 5255.

[3] A.I. Kolesnikov, V.E. Antonov, S.M. Bennington, B. Dorner, V.K. Fedotov, G. Grosse, J.C. Li, S.F. Parker, F.E. Wagner, Physica B 263–264 (1999) 421.

[4] A. Magerl, A.J. Dianoux, H. Wipf, K. Neumaier, I.S. Anderson, Phys. Rev. Lett. 56 (1986) 159.

[5] H. Wipf, in: H. Wipf (Ed.), Hydrogen in Metals III, Springer, Berlin, 1997, p. 51.

[6] A.C. Lawson, A.C. Larson, M.C. Aronson, S. Johnson, Z. Fisk, P.C. Canfield, J.D. Thompson, R.B. Von Dreele, J. Appl. Phys. 76 (1994) 7049.

[7] G. Grosse, F.E. Wagner, V.E. Antonov, T.E. Antonova, Hyperfine Interact. C3 (1998) 221.

[8] V.E. Antonov, B. Dorner, V.K. Fedotov, G. Grosse, A.S. Ivanov, A.I. Kolesnikov, V.V. Sikolenko, F.E. Wagner, J. Alloys Comp. 330–332 (2002) 462.

[9] V.E. Antonov, in: A. Gonis, P.E.A. Turchi, I. Kudrnovsky (Eds.), Stability of Materials, Pergamon, New York, 1996, p. 725.

[10] E.G. Ponyatovskii, V.E. Antonov, I.T. Belash, Usp. Fiz. Nauk 137 (1982) 663. E.G. Ponyatovskii, V.E. Antonov, I.T. Belash, Engl. Transl.: Sov. Phys. Usp. 25 (1982) 596.

[11] V.K. Fedotov, V.E. Antonov, A.I. Kolesnikov, A.I. Beskrovnyi, G. Grosse, F.E. Wagner, Solid State Commun. 107 (1998) 787.

[12] S.V. Vonsovskii, Magnetism, Nauka, Moscow, 1971, p. 618, in Russian.

[13] R.G. Barnes, in: H. Wipf (Ed.), Hydrogen in Metals III, Springer, Berlin, 1997, p. 93.

[14] L.R. Lichty, J.W. Han, R. Ibanez-Meier, D.R. Torgeson, R.G. Barnes, E.F.W. Seymour, C. Sholl, Phys. Rev. B 39 (1989) 2012.

[15] A.V. Skripov, S.V. Rychkova, M.Yu. Belyaev, A.P. Stepanov, J. Phys.: Condens. Matter 2 (1990) 7195.

[16] T. Moriya, K. Ueda, Solid State Commun. 15 (1974) 169.

[17] K. Ueda, T. Moriya, J. Phys. Soc. Jpn 38 (1975) 32.

[18] F. Borsa, R.G. Lecander, Solid State Commun. 20 (1976) 389.

[19] M. Katayama, S. Akimoto, K. Asayama, J. Phys. Soc. Jpn 42 (1977) 97.

[20] H. Nakamura, K. Yoshimoto, M. Shiga, M. Nishi, K. Kakurai, J. Phys.: Condens. Matter 9 (1997) 4701.

[21] Y. Obata, J. Phys. Soc. Jpn 18 (1963) 1020.